

Estimation of the acoustic range of bat echolocation for extended targets

Wolfram-Peter Stilz^{a)} and Hans-Ulrich Schnitzler

Animal Physiology, Institute for Neurobiology, University of Tübingen, Auf der Morgenstelle 28, 72076 Tübingen, Germany

(Received 15 May 2012; revised 12 June 2012; accepted 15 June 2012)

Extended natural structures of the bat environment such as trees, meadows, and water surfaces were ensonified in distances from 1 to 20 m and the echoes recorded using a mobile ultrasonic sonar system. By compensating the atmospheric attenuation, the attenuation of the reflected echo caused by diffraction, energy absorption of the target, and two-way-geometric spreading was calculated for each distance. For each target type the attenuation of the compensated echo sound pressure level was fitted over distance using a linear function which yields simple laws of reflection loss and geometric spreading. By adding to this function again variable atmospheric attenuation, the overall attenuation of a signal reflected from these targets can be estimated for various conditions. Given the dynamic range of a sonar system, the acoustic maximum detection distance can thus be estimated. The results show that the maximum range is dominantly limited by atmospheric attenuation. Energy loss in the reflecting surface is more variable than geometric spreading loss and accounts for most of the differences between the ensonified targets. Depending on atmospheric conditions, echolocation frequency, and the dynamic range of the sonar system, the maximum range for extended backgrounds such as a forest edge can be as short as 2.4 m.

© 2012 Acoustical Society of America. [http://dx.doi.org/10.1121/1.4733537]

PACS number(s): 43.80.Cs, 43.80.Ev, 43.80.Jz, 43.80.Ka [JAS]

Pages: 1765–1775

I. INTRODUCTION

A. Ecological relevance

During evolution the echolocation systems of bats have been adapted to habitat specific echolocation tasks. These tasks depend on where bats navigate in space and search for, find, and acquire food. Comparative studies reveal that the distance to vegetation and ground and the proximity of prey to background targets are relevant ecological constraints on the design of echolocation systems (Aldridge and Rautenbach, 1987; Neuweiler, 1990; Fenton *et al.*, 1995; Schnitzler and Kalko, 2001; Schnitzler *et al.*, 2003; Denzinger and Schnitzler, 2004). If we want to understand how these constraints have shaped the echolocation behavior of bats we should know over which distances bats can detect small prey and also large extended background targets such as rocks, trees, meadows, or water surfaces. In this publication we concentrate on echoes from large targets.

The estimation of maximum detection distances for such targets plays an important role in the discussion of whether the echolocation behavior of bats depends on the detection distance for prey and background targets (Holderied and von Helversen, 2003; Holderied *et al.*, 2006; Jung *et al.*, 2007; Ratcliffe *et al.*, 2011). Some assume that bats keep the pulse intervals long enough, that all background echoes are back before the next call is emitted. Others discuss whether bats alternate between different call

types to prevent ambiguities produced by late echoes from a previous call. For this discussion it is necessary to know the maximal ranges over which bats can perceive echoes from background targets.

Bat echolocation is a sensory system which cannot work over long distances comparable to our visual system. High atmospheric attenuation in the ultrasonic frequency range and two-way geometric spreading loss cause relatively low echo intensities returning to the bat (Griffin, 1971; Lawrence and Simmons, 1982; Hartley, 1989). The atmospheric loss at given environmental conditions and sound frequencies over the distance can be approximated according to ISO 9613-1 (ISO, 1993). There exist models and measurements for the reflection properties of simple solid targets (Kinsler and Frey, 1962; Morse and Ingard, 1968). Using such models, the theoretical maximum detection distance of simple reflectors can be estimated (Griffin, 1971). However, many of the structures of the bat environment are far from being simple solid targets. Until now no good models or measurements over a distance range exist for the reflection intensities of complex natural targets in the bat environment consisting of many statistically distributed reflectors. Because of this lack, only very rough estimates of the bats' maximum detection range for these targets exist.

This research intends to clarify over which distances echolocation enables bats to detect large targets of their natural environment, to quantify echo attenuation of these objects over distance, and to provide a method for the estimation of individual detection ranges depending on dynamic range and frequency of the sonar system, atmospheric conditions, and target type.

^{a)}Author to whom correspondence should be addressed. Electronic mail: peter.stilz@uni-tuebingen.de

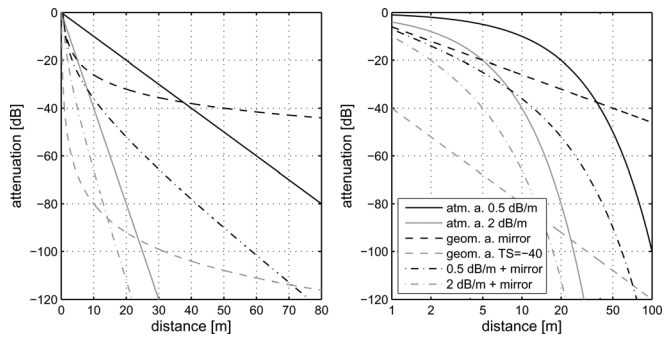


FIG. 1. Atmospheric and geometric components of attenuation for a returning echo. Echo attenuation consists of an atmospheric attenuation component and a geometric spreading loss. The two diagrams illustrate their contribution over distance between reflector and sonar system and differ only in the scaling of the distance axis (linear vs logarithmic). Echo attenuation and spreading loss refer to the source level given for a reference distance of 1 m from the point source. The solid lines depict atmospheric attenuations of 0.5 and 2 dB/m. The dashed lines depict the loss by geometric spreading for reflection at an acoustic mirror and a point reflector with TS of -40 dB. The dashed-dotted lines exemplify the sum of different atmospheric attenuations and the geometric spreading by the acoustic mirror.

B. Theoretical background

The echo to the signal of a sonar system is attenuated by atmospheric and geometric components (Fig. 1).

Atmospheric attenuation is caused by internal friction of the air. At a given frequency and atmospheric condition, a constant proportion of the sound energy is absorbed per traveling distance. Through this, the sound pressure level (SPL) in decibels linearly decreases over distance. Atmospheric attenuation depends on sound frequency, temperature, humidity, and pressure. It can be approximately calculated using ISO 9613-1 (ISO, 1993) (Fig. 2). Since attenuation extremely increases with frequency, the acoustic situation in the ultrasonic range is quite different from our audible frequency range in that acoustic energy is damped out by atmospheric attenuation already at comparatively short distances.

While a propagating wave is permeating an increasing surface, its power is being dispersed, which accounts for geometric attenuation or spreading loss. The intensity leaving a point source is distributed (in the far field) over the surface of a growing sphere whose surface increases according to $A \sim d^2$. This also applies in the far field of a wave emitted by a small directional, anisotropical source (Kinsler and Frey, 1962). Thus, in the emitted spherical wave, the SPL declines by 20 dB per tenfold increase in distance in each direction.

At the boundary of an object in the sound field, part of the emitted energy is scattered and then again subject to spreading loss. The reflected amount of energy and the geometry of intensity distribution within the scattered sound field is affected by geometries of source and reflector and their size relation to wavelength.

If the incoming wave is reflected at an acoustic mirror, the surface of the reflected wavefront keeps growing at the same rate resulting in an overall spreading loss of 20 dB per tenfold increase in distance.

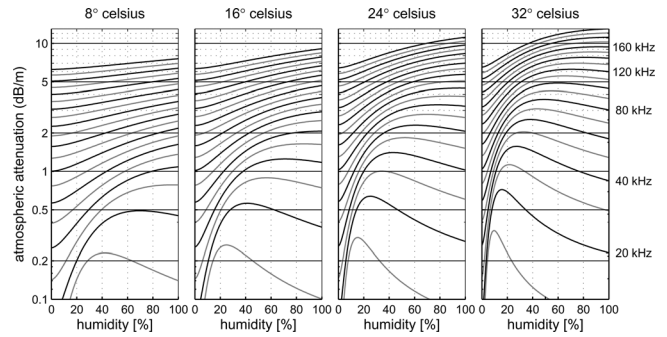


FIG. 2. Atmospheric attenuation in air at temperatures of 8°C , 16°C , 24°C , and 32°C at sea level. Each diagram shows different humidity levels along the horizontal axis for call frequencies of 10–200 kHz (20 frequency lines in 10 kHz steps) the atmospheric attenuation in dB per meter at 101 325 Pa (calculated according to ISO 9613-1).

If the wave is reflected at a small reflector, the incoming intensity at the reflector decreases with distance at -20 dB per tenfold increase in distance, and causes another spherical wave to be emitted with a certain reflected sound power which is once more spread, resulting in an overall two way spreading loss of 40 dB per tenfold increase in distance. Since a literal point reflector has no area and thus reflects no energy, we consider small reflectors where spherical spreading of sound power can be assumed. Spherical spreading can be assumed in the sound field reflected by an object where: (a) the distance from the object is much larger than maximum object diameter ($d \gg D$), which ensures that all reflected elementary waves spread at the same geometric rate, (b) the distance from the object is much larger than the wavelength ($d \gg \lambda$), where phase relations within the spreading wave are constant, and (c) the Fraunhofer condition ($d \gg D^2/\lambda$) is satisfied, which certifies that phase shifts of all reflected superposing elementary waves stay constant during further propagation. The scattered sound field of such a small reflector still does not have to be homogeneous or omnidirectional, but the scattered intensity decreases in each direction by 20 dB per tenfold increase in distance.

The limited size of a small reflector scatters only a part of the sound power of the primary wave. The amount can be quantified by a target strength (TS) which specifies the ratio of sound intensity of the reflected wave in a reference distance (e.g., re 1 m) to the sound intensity incident at the object. A TS of -40 dB indicates that the reflected sound wave in 1 m distance of the target is 40 dB weaker than the sound wave incident at the target.

For a constant target shape and fixed ratio of reflector size to wavelength λ , the reflected sound power is proportional to the area covered by the target in the sound field (Kinsler and Frey, 1962; Skolnik, 2001).

The proportion of the reflected sound power and thus TS also depends on the ratio of wavelength λ to reflector size. In the Rayleigh region, where the reflector size is much smaller than wavelength (Rayleigh, 1896), most energy is diffracted around the target. The intensity reflected by a small sphere decreases with wavelength according to $I \sim 1/\lambda^4$. In the geometric region, where the reflector size is much larger than wavelength (Skolnik, 2001), the sound

power of the incident wave which permeates the cross-section area of the target is reflected independent of wavelength. However, the distribution of sound intensity in the reflected field (e.g., back to the sonar system) can range from omnidirectional to very jagged or directional depending on reflector geometry, orientation, and size ratio to wavelength. In the resonance region, where the reflector size is in the order of wavelength (Skolnik, 2001), the reflected power of a sphere oscillates with increasing wavelength in the range of the power of the sound field permeating the area of the target.

A solid sphere of 4 cm diameter, for example, has in the geometric region ($\lambda \ll 4\pi$ cm) a TS of -40 dB (Kinsler and Frey, 1962), in the resonance region ($\lambda \approx 4\pi$ cm) approximately -40 dB, and in the Rayleigh region ($\lambda \gg 4\pi$ cm) the TS is strongly decreasing with wavelength.

In the process of reflection, energy can also be transmitted through, or be absorbed by, the target. The loss depends on reflector rigidity and acoustic densities of the involved media. If sound energy is transmitted through a vibrating or porous reflector, or absorbed by its material, only a reduced proportion of the incident energy is scattered back to the sonar system (Kinsler and Frey, 1962). For the receiving sonar system it is not important as to whether a reflector absorbs energy or scatters it away.

Atmospheric attenuation increases linearly with reflector distance, and geometric spreading reduces echo level per tenfold increase in distance by 20 dB for the acoustic mirror and by 40 dB for the point reflector (Fig. 1). For targets whose size and geometry is intermediate between an infinite plane and a small reflector, spreading loss would be expected to be between those extremes. If only a small fraction of energy is reflected, the echo level is shifted downward by a constant offset. For point reflector, the offset corresponds to its TS (e.g., -40 dB). Similarly, if only a small part of the incoming energy would be reflected and most of the energy absorbed by a mirror-shaped reflector, the echo's geometrical attenuation line would be shifted downward. A loss of 99% of the energy would result in a 20 dB weaker reflection and downward shift. The sum of atmospheric attenuation and geometric spreading loss (including the vertical offset) results in the overall echo attenuation, while at short distances the echo attenuation is mainly determined by the geometric spreading loss (inclination of geometric spreading line), or energy absorption of the target or TS (its vertical offset), at large distances atmospheric attenuation is clearly overtaking.

C. Our approach

In our research we recorded the echoes produced by complex targets with an artificial sonar system and measured the echo attenuation in different distances under known atmospheric conditions. The atmospheric part of attenuation was calculated and compensated in the gathered data. The remaining attenuation caused by geometric spreading, scattering, and energy absorption of the reflector were altogether treated as a generalized geometric attenuation (GGA). The GGA-function over distance is dependent on the reflection

properties of the target and also wavelength, but not on atmospheric conditions.

Because of high atmospheric attenuation and reduced sensitivity of our artificial sonar system at high frequencies, the dependence of the GGA on frequency was calculated at short distance echoes for each target. Subsequently the GGA was studied over all distances for a wideband sweep with its spectral peak at 50 kHz.

For the calculated GGAs of a target over distance, the parameters C_1 and C_2 of the function $\Delta L(d) = C_1 + C_2 \cdot \log_{10}(d/d_{\text{ref}})$ as a simple GGA model were extracted by linear regression. This regression function models reflection loss and spreading geometries of the echo evoked from a small sonar sound source. ΔL describes the SPL loss of the returning echo (at the receiver) relative to the emitted signal (measured in 1 m reference distance in front of the emitter) over the distance d of the sonar system to the target. d_{ref} is the reference distance (1 m), where the reference SPL of the source was measured.

C_2 quantifies the loss due to energy spreading on the way forth and back, which depends on the geometry of the reflected wave, which is affected by the size and geometry of the target. A large flat plane would yield $C_2 = -20$ dB caused by the spherical propagation from the sound source, which is just mirrored by the reflector. For a point reflector $C_2 = -40$ dB, which is the sum of two times -20 dB geometrical attenuation of the spherical waves initiating from the sound source and again from the small target. For both reflectors, spreading loss increases linearly over the logarithm of distance (Fig. 1, right). For long tubular structures, $C_2 \approx -30$ dB would be expected.

C_1 accounts for the fraction of energy reflected. This is determined by target size and sound absorption or transmission of the reflector. A perfect acoustic mirror would yield $C_1 = -6$ dB, because the reflected spherical wave has to travel twice the reference distance d_{ref} when $d = d_{\text{ref}}$ and lose 6 dB by geometric spreading on the way back, therefore is 6 dB weaker than the reference SPL of the sound source. If 99% of the incoming energy is absorbed by this plane, C_1 would decrease by the loss of 20 dB. If the target can be approximated as a point reflector, C_1 represents and equals its TS (re 1 m). A solid sphere of 4 cm diameter has, for small wavelengths, approximately a TS of $TS = -40$ dB re 1 m (equivalent to $TS = -20$ dB re 10 cm).

In our model, simple reflectors would be represented by GGA-functions $\Delta L(d) = C_1 + C_2 \cdot \log_{10}(d/d_{\text{ref}})$.

	C_1	C_2
Small reflector	TS	-40
Mirror	-6	-20
Lossy plane	$-6 - \text{loss}[\text{dB}]$	-20

Using the resulting GGA functions, it is possible to add again the atmospheric attenuation of given conditions and thus estimate the overall attenuation in arbitrary environments. Moreover it is possible to estimate the overall attenuation in distances to the targets, which could not directly be measured because of the limited dynamic range of the technical sonar system used. By comparing the dynamic range of

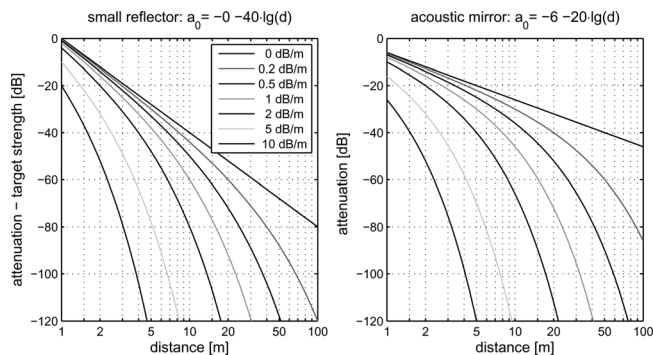


FIG. 3. Theoretical attenuation of echoes from simple targets. The diagrams show the theoretical overall echo attenuation after reflection at a small reflector and an acoustic mirror for different atmospheric attenuations. Left: Small reflector. The object's individual TS has to be added as a vertical offset. A TS of -40 dB (re 1 m) would cause an additional constant attenuation (or line downward shift) of 40 dB. Right: Acoustic mirror.

a bat's sonar system between sound emission level and auditory threshold with the overall attenuation of the echoes in different distances, it is possible to estimate also the maximum detection range of the ensonified backgrounds under arbitrary conditions.

The overall attenuation and maximum detection range of planes and small reflectors can be constructed using Figs. 2 and 3. Atmospheric attenuation depending on frequency and atmospheric conditions can be read from Fig. 2. Atmospheric attenuations from 0–10 dB/m are added to the GGA functions in Fig. 3. A sonar system with a source level of 100 dB SPL in 1 m distance and an auditory threshold of 20 dB SPL has a dynamic range of 80 dB. To read its maximum detection range of a small reflector with $TS = -40$ dB the additional TS loss can be subtracted from the dynamic range of 80 dB. This leaves 40 dB of further attenuation. This is met for the -1 dB/m atmospheric attenuation line at approximately 5 m. For detecting the non-lossy ($C_1 = -6$ dB) acoustic mirror by the same sonar system and atmospheric conditions, the dynamic range of 80 dB will be used up by attenuation at a maximum detection distance of approximately 24 m. If a mirror-shaped structure reflects only 1% of the incoming energy (-20 dB further loss), the range is limited to approximately 15 m.

II. MATERIALS AND METHODS

A. Data acquisition

1. Examined targets

Four vertical and two horizontal background targets were ensonified using a mobile sonar system. The vertical background targets were large pear trees, a leafy forest edge, a telegraph pole of 0.3 m diameter, and a large concrete wall. The horizontal background types were a meadow and the nonturbulent water surface of a slowly flowing river.

2. Sonar system

The mobile sonar system consisted of a sonar head with a loudspeaker flanked by two microphones, a mobile GNU-

Linux-PC with one one-channel D/A-card, and one two-channel A/D-card which were connected to the amplifiers of the sonar head and a portable power supply.

As transducers of the loudspeakers and microphones Polaroid 600 (4 cm diameter) were used. The microphones were mounted 6 cm (axis to axis) aside the loudspeaker in parallel orientation. All electronic circuits and amplifiers of the sonar head were designed and built in the electronic laboratory of the Department of Animal Physiology, University of Tübingen. The system had a bandwidth of 20–150 kHz. The maximum intensity of 112 dB [SPL root-mean-square (rms)] in 1 m distance was reached at 50 kHz; the wideband noise of the recording system was approximately 25 dB (SPL rms) with peaks at 35 dB (SPL). The main beam intensity of the transducers at 50 kHz dropped 30 dB at 15° off axis.

The GNU-Linux-PC was equipped with a Gage Compu-gen 1100 1MB D/A-card for signal generation and a 2-channel Gage Compuscope 512 PCI 1MB A/D-card for data acquisition. Custom-written ensonification software generated arbitrary signals, and converted them at a sampling rate of 10 MHz in the D/A-card for reproduction by the sonar head. The incoming signal was digitized at a sampling rate of 1 MHz and stored on the hard disk for analysis. Vertical resolution was 12 bits each way.

The portable power supply was fed by a large 12 V battery. Voltage was converted for providing the mobile PC and the amplifiers with power and the transducers with 200 V polarization voltage.

As ensonification signal a linear sweep was used, falling within 4 ms linear from 140 to 25 kHz and reaching in 1 m distance a peak of 112 dB (SPL rms) at 50 kHz.

The sonar head was mounted in 3 m height on a lengthened tripod for ensonification of the vertical targets. For ensonification of the horizontal targets it was lowered, hanging vertically on a crane-like structure from a bridge crossing a river and a meadow.

3. Ensonification

The sonar system was positioned in 10 equally spaced distances of 2–20 m to the vertical backgrounds and in 10 equally spaced heights of 1–10 m above the horizontal backgrounds. The distance was defined as the closest distance to the most dense area in the target surface. The sonar head was always oriented frontally toward the targets. For the vertical backgrounds the sonar head was lifted in a height of 3 m to avoid ground reflections, and for the horizontal backgrounds the sonar head was vertically lowered from a bridge.

For each recording situation (same target and distance) 50 two-channel echoes of different sonar head positions were recorded. For comparison of the overall geometric attenuation of the echoes with the simple law of the one-way geometric spreading of sound emerging from a small source and as a calibration measurement, loudspeaker and microphones were separated and the emitted sweep was directly recorded in 12 equally spaced distances from 1 to 12 m of the loudspeaker in a noise-attenuated sound chamber. For

noise measurements, under all conditions described above, the background noise was additionally recorded with the same recording system settings without ensonification signal output. For obtaining the emitted reference signal, the emitted signal was recorded in 1 m distance in front of the loudspeaker with a microphone of the sonar head. During all recordings, temperature and humidity were measured for individual compensation of the atmospheric attenuation.

B. Data analysis

All data analysis was done in MATLAB on a GNU-Linux system.

1. Preprocessing and analysis window

To avoid the effects of frequencies outside the sonar systems range, all acquired data was initially bandpass filtered with an elliptic fourth order bandpass filter of 10–300 kHz. For easier and continuous amplitude analysis all signals were thereafter converted into analytic signals by Hilbert transformation.

For each recording distance a time window was defined which corresponded to an echo generation distance of any signal part from 1 m before to 5 m within the vertical targets and from 0.5 m before to 2.5 m within the horizontal targets. For the direct recording calibration the time window corresponded to 0.5 m before to 2.5 m divided by sound speed behind the signal expectation time. Of each echo recording only the content of this time window was used for analysis.

2. Spectral effect of scattering

In echoes recorded in farther distances, the high frequency content of the echoes was subsequently superimposed by noise, which prevented spectral analysis in large distances. The critical frequency and distance range depended on the target.

For each echo recording in 2 m distance (vertical targets) or 1 m (horizontal targets and calibration) the power spectral density (PSD) over the selected time window with a resolution of 4 kHz was estimated and compared to the PSD estimate over a time window of the same length of the corresponding noise recording. From this, the coherent frequency range in which all echo recordings of a target type exceeded noise recordings by at least 3 dB was selected. The obtained PSDs were spectrally compensated for atmospheric attenuation over the corresponding range at atmospheric conditions. Of the resulting compensated spectra the spectrum of the reference sweep was subtracted in decibel domain. The resulting function resembles the difference of reflected and incident spectrum at the target with atmospheric attenuation eliminated, which can be interpreted as the spectral filter at reflection or target color.

In order to quantify the spectral filtering effect of scattering, for each target type a linear regression over the selected frequency range was calculated of all obtained difference spectra averaged. A negative inclination of the linear regression function indicates a stronger loss in high frequencies. As a measure of the regression quality, for each target

type the rms error of the residuals of the individual difference PSDs to the linear regression model was calculated.

3. Overall echo attenuation

For all echo recording samples of each target and distance, the energy contained in the previously defined analysis window was extracted as well as the peak amplitude within this window. The values of all echoes of the same situation (target and distance) were averaged.

The same parameters were calculated for this situation's noise recording. Only those distances were further analyzed in which the mean of the energy and respective peak parameters was at least 3 dB higher than those of this situation's noise recording.

Of the obtained echo energy and peak parameters, the average energy or peak parameter of the corresponding noise recordings was subtracted. This compensation of noise contribution allows an extrapolation of the attenuation function in decibel domain in distances, in which the parameter exceeds only slightly the noise parameters. Otherwise, after logarithmizing the values to dB-scale, the logarithmized echo attenuation functions over distance would, where only slightly above noise, become asymptotical to the noise line in these cases and useless for interpolation. The direct calibration recordings were processed analogously.

4. Generalized geometric attenuation (GGA)

The emitted reference sweep was exactly cut out of the reference recording based on the cross correlation with the digital signal. Then it was first algorithmically compensated for atmospheric attenuation in the reference recording distance by multiplying it based on its known linear time-frequency-structure with a function inverting the atmospheric attenuation of each frequency at the reference recording situation. Afterwards it was again algorithmically attenuated by multiplying its known linear time-frequency-structure by functions simulating atmospheric attenuations of all recording distances and atmospheric conditions of the echo recordings. The resulting sweeps were embedded in windows of zeros of the same length as the echo analysis windows. Energy and peak contained in these windows were extracted. The ratios of the corresponding parameters of the echo recordings to the parameters of the simulated atmospherically attenuated sweep were calculated. The resulting ratio was logarithmized and converted into decibels. By this procedure, the atmospheric part of echo attenuation was compensated. The remaining attenuation of echo parameters is caused by geometric spreading, scattering, and energy absorption, which is treated as a GGA.

The resulting attenuations in decibels over logarithm of distance were averaged for each target type and used for linear regressions of the parameters C_1 and C_2 in the function $\Delta L(d) = C_1 + C_2 \cdot \log_{10}(d/d_{\text{ref}})$.

5. Range of bat echolocation

With the resulting GGA regression functions, the overall attenuation caused by scattering, absorption, and geometric

spreading for arbitrary distances can be interpolated. By adding again the atmospheric attenuation of arbitrary atmospheric conditions and sound frequencies, the overall attenuation can be calculated. For a known frequency and a known dynamic range of a bat's sonar system between sound emission level (in reference distance) and auditory threshold, this overall attenuation function can be used to calculate over which distances the examined backgrounds will return an audible echo of the emitted signal to the bat.

III. RESULTS

A. Spectral effect of scattering

In the frequency range of 20–120 kHz the PSDs of all echoes of all backgrounds were well above noise in the shortest recording distance. The inclinations of the linear regression functions of the difference spectra between the attenuation-compensated reflected spectra and the emitted spectrum in this range were between +0.03 and -0.14 dB/kHz. The rms error of the regression functions to the individual difference spectra over the range of 20–120 kHz was 4.2 dB for the forest and maximal 2.6 dB for all other backgrounds (Table I).

The result indicates that the targets filter the reflected spectrum to a certain extent. The natural targets absorb or scatter some of the higher frequencies.

B. Overall echo attenuation

In the vertical targets the peaks of the echo are well above noise level up to distances from 10 m (tree, forest edge) to 20 m (wall, Fig. 4, left). In the horizontal targets, the echo peaks were not buried in noise up to the maximum distance recorded of 10 m (Fig. 5, left).

Already at the shortest distances, the echo peaks of leafy targets start far below the signal peak, which indicates that a large part of the incoming intensity has not been reflected back in the direction of the sonar head.

C. GGA

Corresponding to the overall attenuations, the GGA of the leafy targets exhibit high losses compared to the signal level already at shortest distances. The intensity then decreases in most cases approximately linear over logarithm of distance with a moderate inclination of approximately -20 dB per tenfold increase in distance (Figs. 4 and 5, right).

The direct propagation recording of the emitted sweep was processed analogously. The resulting GGA-function also shows an approximately linear decay over logarithm of

TABLE I. Linear regression of target spectral filtering 20–120 kHz.

Target	Inclination [dB/kHz]	rms ϕ [dB]
Forest	-0.13	4.2
Tree	-0.14	2.6
Pole	+0.03	1.7
Wall	-0.08	2.1
Water	-0.04	2.5
Meadow	-0.11	2.5

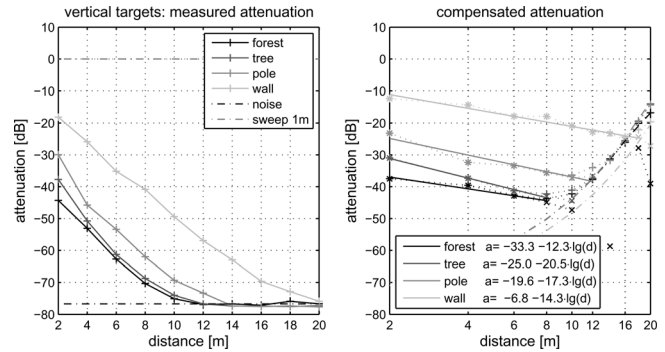


FIG. 4. Echo attenuation and GGA of the vertical targets. Left: Mean echo peak relative to the emitted signal peak level (in 1 m distance) over target distance. The lower horizontal line denotes the noise peak level of noise recordings. Right: Mean echo peak GGA obtained by compensation of atmospheric attenuation. In \times -marked points the noise contribution to the signals energy has been compensated while $+$ -marked points are not corrected for noise contribution. The solid lines indicate the GGA interpolation. The lower dashed-dotted lines display the noise floor as the GGA that would be extracted from the noise recording.

distance with an constant inclination of approximately -20 dB per tenfold increase in distance (Fig. 6).

Diagrams showing echo energy decay over distance instead of echo peak decay look very similar in shape, though the distance to noise is slightly lower and their parameters approximate the noise line at shorter distances.

D. Interpolated GGA functions

Using the data of echo attenuation caused by spreading and reflection over the distance of a linear regression of GGA functions for the energy and peak parameters (in decibels) resulted in the function parameters shown in Table II.

Table II also shows the attenuation function for the control calibration measurement of simple spherical wave propagation. For comparison, the last three lines of Table II show theoretical values for simple spherical wave propagation and for reflection at an acoustical mirror and a point reflector with the TS.

The different backgrounds exhibit remarkable differences in the vertical offset (C_1) of the peak attenuation functions (1 m reflector distance) varying in vertical backgrounds from -33.3 dB (forest) to -6.8 dB (wall) and in horizontal backgrounds from -20.1 dB (meadow) to -4.4 dB (water). The functions' inclinations (C_2) vary much less, all lying in

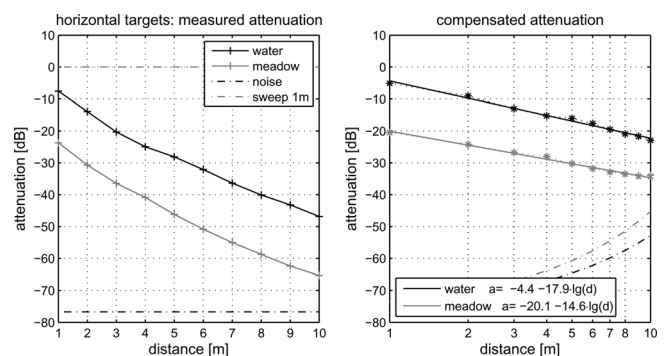


FIG. 5. Echo attenuation and GGA of the horizontal targets.

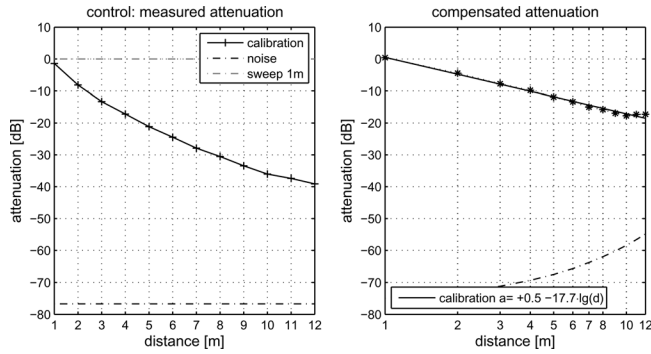


FIG. 6. Spherical propagation attenuation and GGA of the control measurements. Left: Mean peak level relative to the emitted signal peak level (in 1 m distance) over target distance. Right: Mean peak GGA.

the range of -20.5 dB to -12.3 dB per tenfold increase in distance for the peak parameter. Surprisingly, most inclinations are shallower than the inclination which would be expected for a mirror-like reflector.

E. Estimation of maximum echolocation range

By adding variable atmospheric attenuations to the peak GGA regression functions, for the ensonified backgrounds the overall echo attenuations at arbitrary atmospheric conditions and distances can be calculated (Figs. 7 and 8). For comparison, the corresponding diagrams for a point reflector and an acoustic mirror are provided (Fig. 3). Using these diagrams, it is possible to estimate the overall echo attenuation over distance for variable atmospheric attenuations. The atmospheric attenuations can be estimated according to the atmospheric conditions (Fig. 2). Through this, it can also be estimated over which distance the echoes to a signal of a certain source level will return above and below auditory threshold. The actual maximum echolocation range depends

TABLE II. GGA functions.

$\Delta L(d) = C_1 + C_2 \cdot \log_{10}(d/d_{ref})$				
Parameter [dB]	Peak		Energy	
	C_1	C_2	C_1	C_2
Vertical backgrounds				
Forest	-33.3	-12.3	-34.6	-6.5
Tree	-25.0	-20.5	-27.4	-14.3
Pole	-19.6	-17.3	-21.5	-17.1
Wall	-6.8	-14.3	-8.0	-13.7
Horizontal backgrounds				
Water	-4.4	-17.9	-5.0	-18.3
Meadow	-20.1	-14.6	-23.2	-13.4
Calibration				
Propagation	0.5	-17.7	-0.8	-16.9
Theoretical targets				
Propagation	0	-20	0	-20
Mirror	-6	-20	-6	-20
Point reflector	TS	-40	TS	-40

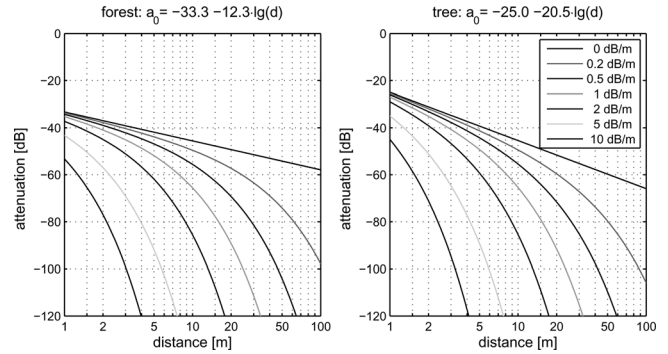


FIG. 7. Extrapolated attenuation for vertical targets. The diagrams show the extrapolated overall echo attenuation over target distance according to the GGA model $\Delta L = C_1 + C_2 \cdot \log_{10}(d/d_{ref})$ and different atmospheric attenuations. Compared to the acoustical mirror (Fig. 3, right) the vertical offset of the cohort of attenuation lines is very conspicuous. This is due to the loss of energy in the depths of these targets compared to the acoustical mirror. A sonar system of 80 dB dynamic range at an atmospheric attenuation of 1 dB/m would achieve in both cases a maximum detection range of approximately 15 m. Left: Forest edge. Right: Large tree.

for each target on the parameters temperature, humidity, call frequency, and dynamic range of the sonar system.

IV. DISCUSSION

A. Spectral effect of scattering

The linear regressions of the difference spectra between attenuation-compensated reflected spectra and the emitted spectrum exhibit a slight, in most cases, negative inclination. An inclination of approximately -0.1 dB/kHz implies that, relative to the emitted spectrum, echo levels are during reflection at 80 kHz by approximately 3 dB are more attenuated than at 50 kHz, where the energy of the ensonification sweep was centered. There seems to be a tendency of spectral low pass filtering during the reflection, especially at the leafy targets. Compared to the dynamic range of sonar systems and of approximately 100 dB, the filtering impact does not constitute a very significant part of the maximal overall echo attenuation. Therefore, and for

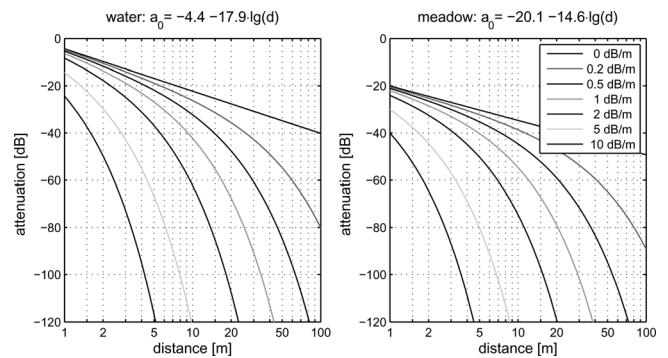


FIG. 8. Extrapolated attenuation for the horizontal targets. Left: Water surface. The water surface resembles very closely an acoustical mirror (Fig. 3). Right: Meadow. The meadow resembles a lossy acoustical mirror. The inclination of the geometrical attenuation model function is nearly the same as the inclination of the function modeling the water surface reflection, just the vertical offset is 15 dB lower (see also Fig. 5) which is caused by energy loss in the reflecting surface. The example sonar system defined in Fig. 7 would have a maximum detection range of 24 m for the water surface and 20 m for the meadow.

keeping the estimation simple, the estimations of echo attenuations presented below do not account for spectral filtering during reflection.

If the estimation of echo overall attenuation should also consider the spectral filtering of the reflection, this could still be done by adding the targets' spectral filtering difference (which can be calculated from Table I) of the actual frequency to the center frequency of 50 kHz of the ensonification sweep.

The moderate rms-errors of the linear regressions to the actual difference spectra indicate that the linear regression is a reasonable approximation for the spectral filtering from where no substantial deviation in relation to the dynamic range of the sonar system must be expected.

B. The linear model for GGA

The data presented in this paper is pragmatically aimed at estimation of distances, over which bats can perceive echoes of extended targets in their natural environment under variable conditions.

The linear regression GGA-function $\Delta L = C_1 + C_2 \cdot \log_{10}(d/d_{\text{ref}})$ for approximation of the echo attenuation by geometric spreading, scattering, and energy absorption has been chosen because this simple function correctly models the attenuation caused by a variety of simple reflector geometries in a limited distance range.

However, for an adequate description over a wide distance range, the reflector model and the linear approximation function have to be adapted. A reflector with a geometry of a very large sphere acts in extreme proximity rather like a plane mirror-like reflector, though in extreme distances, any reflector of limited size becomes a small reflector. One simple linear model cannot correctly describe this transition for all distances. The situation for an extended reflector composed of many small surfaces over a reflection depth is even more complicated. Under this aspect, the linear modeling function cannot be regarded as a physical rule which can generally describe the reflection properties for any given distance, but rather as a simple linear approximation which gives a usable reflection description for a limited distance range. The compensated data shown in Figs. 4, 5, and 6 (right parts) suggest that a linear approximation is sufficient for regression in the recorded range.

No exact physical model which explains the complex reflection properties for the ensonified extended targets is given in this work. The offset C_1 generally quantifies the proportion of the incident energy, which is reflected back toward the sonar system. For a target with sparse surface density, small reflection area, adverse surface orientations or damping consistence, this proportion will be low. For small targets causing a spherical reflected wave, this offset indicates the TS. The inclination C_2 describes the geometry of energy spreading at reflection, taking also into account the spherical energy spreading of the emitted signal. For flat surfaces, C_2 would be -20 dB, for small reflectors causing another spherical wave, C_2 would be -40 dB, for convex mirrors focusing the incident energy back to the emitter, C_2 could also be higher than -20 dB.

C. GGA-functions of the examined targets

For the large plane reflectors meadow and water, we expected a mirror-like behavior ($C_2 \approx -20$ dB). The water surface parameters approximately resemble an acoustical mirror with a somewhat smaller intensity decay C_2 over distance. The meadow parameters roughly resemble a lossy acoustical mirror with a significantly smaller intensity decay over distance. In both cases, the smaller decay could be correlated to the not completely smooth surface which could have some cat-eye-like focusing effect, which would be stronger in the meadow with a surface composed of countless leaves of grass.

The tree and the forest exhibit a large negative offset C_1 , indicating a small proportion of energy reflected back and a large energy loss in the depth of vegetation.

The low intensity decay C_2 per tenfold increase in distance of the targets of -12.3 to -20.5 dB for echo peaks is intuitively surprising. The singular low value of $C_2 = -6.5$ dB for the energy parameter at the forest edge is probably caused by the singularly short distance in which the parameter in this setting exceeded noise, which allowed CGA interpolation only over three distances. For an infinite flat surface -20 dB would be expected, and for a target of limited size, this figure would be rather more negative. However, the distances over which most echoes could be recorded were less than the overall target size. In this range, the limited target size could not have a prominent impact on the echo decay over distance to cause a more point-reflector-like behavior. Conversely, for the leafy targets, the small reflectors were distributed over a reflection depth behind the target's surface. Because of this, the echoes were generated on average in a larger distance than the defined distance to the target's surface. This additional reflection depth behind the target's surface is relatively large for small target distances but becomes relatively small for large target distances. Through this, the echoes recorded at small distances are produced in (variable) over proportional increased distances and are thus over proportionally more geometrically attenuated. Thus the echo decay function interpolated over target distance (defined by surface distance) becomes rather less steep. Another possible explanation for low intensity decay over distance from the leafed targets is the composition of many small flat reflectors which could statistically often form angular cat-eye-like structures which preferably reflect the incident sound back to the source, rather than scattering it homogeneously away in all directions. This could give those targets a rather flat-reflector-like or even focusing acoustic behavior. The wall also did not have a smooth surface, but an irregular rough surface with protrusions of approximately 3 cm, which could have produced similar effects.

The inclination of the tubular pole's echo attenuation is surprising low. Petrites *et al.* (2009) ensonified long chains used within an experimental setup and compared their echo decrease over the target range with echoes of small targets such as spheres and mealworms. They also found a remarkably low decrease of chain echo strength in the range from 20 to 140 cm.

Griffin and Buchler (1978) examined the reflections of large natural horizontal surfaces such as grass and bushes in

the frequency range of 1–6 kHz. Assuming mirror-like spreading, reflection loss was defined as the excess loss compared to the expected reflection by a perfect mirror, from which returning echoes would be 6 dB weaker than the intensity incident at the mirror ($C_1 = -6$ dB). The measured reflection losses increased with frequency and reached at 6 kHz 13.0 dB (grass) to 16.8 dB (bushes). This corresponds to C_1 of -19 dB to -22.8 dB. If we assume some further increase with frequency, these losses are similar to our results.

D. Estimation of maximum echolocation range

Bat species use a wide range of frequencies for echolocation. The atmospheric conditions under which they echolocate in their diverse habitats span an extremely wide range of temperature and humidity. Ecological constraints and environmental conditions force compromises in the design of echolocation systems (Griffin, 1971). The distance to prey and to background targets such as vegetation and ground are relevant ecological constraints (Aldridge and Rautenbach, 1987; Neuweiler, 1990; Fenton *et al.*, 1995; Schnitzler and Kalko, 2001; Schnitzler *et al.*, 2003; Denzinger and Schnitzler, 2004). Only if we know over which distances bats can detect small prey such as flying insects and also large extended background targets such as buildings, rocks, forest edges, trees, meadows, or water surfaces, can we test the hypotheses of how the constraint target distance has shaped the echolocation systems of bats during evolution.

The echolocation range is limited to distances over which the returning echoes to the emitted signal after spreading, scattering, absorption, and atmospheric attenuation exceeded the auditory detection thresholds. The maximum distance of this range is reached when the echo level equals the detection threshold.

In decibel domain, source level can be called SL and detection threshold can be called DT. Echo attenuation relative to SL (including full 2-way-transmission loss) can be called EA. Thus, the maximum detection range condition from above can be put as $DT = SL - EA$. If we define the dynamic range (DR) of a sonar system as $DR = SL - DT$, the condition is $DR - EA = 0$. For estimating the maximum detection distance of a sonar system, one therefore needs to know the system's DR defined by SL and DT and the EA as a function of target distance.

There have been many attempts to estimate maximum detection distances [e.g., Holderied and von Helversen (2003); Jung *et al.* (2007); Ratcliffe *et al.* 2011] by using the sonar equation (Urlick, 1983; Mohl, 1988). However, the sonar equation as used by Urlick (1983) and Mohl (1988) $DT = SL - 2TL_1 + TS$, where $2TL_1$ denotes two times the one-way-transmission loss TL_1 , cannot be applied on the general case including large targets because the equation is based on a TS and implies spherical spreading of emitted wave and of the reflection and a two-way-geometric spreading loss of 40 dB per tenfold increase in distance. This is generally not the case (i.e., in the proximity of large targets), but only valid for the special case of small targets with point-reflector-like behavior. Generally the concept of just doubling the one-way-transmission loss for obtaining the

two-way-transmission loss is not applicable if the geometry of the reflected wave differs from the spherical geometry of the emitted wave.

The EA (including two-way-transmission loss) can be separated in EA_A caused by atmospheric attenuation and EA_G caused by spreading, scattering, and absorption. $EA = EA_A + EA_G$ and thus at maximum detection distance $DR - EA_A - EA_G = 0$.

The atmospheric attenuation is reasonably understood and thus EA_A can be approximately calculated for given atmospheric conditions and distances according to ISO 9613-1 (ISO, 1993).

The attenuation caused by spreading, scattering, and absorption (EA_G) has been measured in this research for various backgrounds and linearly modeled as the GGA-function over distance: $-EA_G \approx \Delta L = C_1 + C_2 \cdot \log_{10}(d/d_{ref})$ with the parameters C_1 and C_2 . This function includes the special case of small point reflectors for $C_2 = -40$ and $C_1 = TS$.

Since the targets generally return no perfect copy of the emitted signal, the attenuations of different signal properties can be examined. While different parameters such as echo energy within a time window, or outputs of a matched filter could also be considered, this research focuses on the echoes peak amplitude because this parameter in relation to auditory threshold implies the clearest physiological restriction to detection. If the echo peaks return below auditory threshold, the auditory system will not be able to perceive, and no later mechanism such as matched filters will be able to detect the echo. Conversely, if the echo would only be buried in noise, matched filters could help to detect its presence. Other parameters such as echo energy contained in a time window showed a similar behavior over distance like the echo peak, but echo energy tends to be buried in noise over shorter distances.

The measurement of the SL of echolocation signals is only possible if the directional sonar beam of the bat points to the measuring microphone and if the directional microphone points to the bat. Additionally, distance between the bat and microphone and air temperature and humidity have to be known so that the amount of atmospheric attenuation can be calculated. Only a few measurements in the field fulfill all these conditions. Surlykke and Kalko (2008) investigated tropical edge and open space foragers and found SLs (related to a distance of 10 cm from the bats mouth) of 122–134 dB. Holderied and von Helversen (2003) report for European edge and open space foragers SLs (related to a distance of 10 cm from the bats mouth) a rather similar range of 121–131 dB. The reported SL values are 20 dB lower if a standardized SL definition distance of 1 m from the sound source is used.

The DT of flying bats while performing a specific echolocation task is difficult to measure. Only if TS in the experiment, DR, and the SL of the used signals are known is it possible to estimate the DT. In earlier studies with flying bats (summarized in Schnitzler and Henson, 1980), Griffin (1958) estimated a DT of 17 dB for *Eptesicus fuscus*, detecting a spherical object at a distance of 2 m and Griffin *et al.* (1960) determined a DT of 15–30 dB in *Myotis lucifugus* catching fruit flies. In bats avoiding obstacles, a DT of 23–28 dB was calculated for *Myotis lucifugus* (Griffin, 1958), of 25–34 dB for *Rhinolophus ferrumequinum* (Sokolov, 1972), and of

9.2–21.6 dB in *Myotis oxygnathus* (Ayrapetyants and Konstantinov, 1974). Most of the estimated DTs were in the range between 15 and 30 dB. In psychophysical experiments with stationary bats the estimated DTs ranged between 0 and 59 dB SPL at detection distances between 0.12 and 5.1 m (summarized in Moss and Schnitzler, 1995). High DTs above 30 dB may result from the middle ear reflex which is effective at short target distances and also from masking clutter in a narrow experiment chamber. The lowest DT of 0 dB was determined by Kick (1982) for well-trained *Eptesicus fuscus* when detecting a single real target which was offered at a distance of 5.1 m far from a clutter producing background. From all these experiments we conclude that the DTs of bats flying under natural conditions may be somewhere around 20 dB, and that it is unlikely that bats have a DT of 0 dB as assumed in some publications (e.g., Holderied and von Helversen, 2003). Under the assumption that the DTs of free flying bats are at approximately 20 dB (see above) and that the SLs (related to 1 m) of edge and open space bats range between 101 and 111 dB (according to Holderied and von Helversen, 2003), we can estimate the DRs of the echolocation system of bats. These DRs range between 81 dB in smaller edge space foragers with lower SLs and higher frequencies and 91 dB in larger open space foragers with higher SLs and lower frequencies.

Knowing the DR and the frequency of a sonar system and the atmospheric conditions, we can use our data (C_1 and C_2) to estimate the overall attenuation of the echo over distance and the sonar systems DR and thus the maximum detection distance.

Maximum detection ranges can be estimated based on this research as exemplified in the following: A bat producing 120 dB at a certain frequency in 10 cm distance in front of the mouth yields a source level of 100 dB in 1 m distance of the sonar system. If the call frequency used is 35 kHz and the auditory threshold is 20 dB for this frequency, the bats dynamic range spans 80 dB for this frequency. If the ambient temperature is 16 °C and the relative humidity is 80%, the call frequency of 35 kHz is atmospherically attenuated at a rate of 1 dB/m (Fig. 2). Under these conditions, the echo of a tree or forest edge would be farther attenuated than the systems dynamic range of 80 dB at distances greater than 15 m, meaning that the echo will return below the auditory threshold of the bat (Fig. 7). If a large insect with TS of –40 dB re 1 m (corresponding to a TS of –20 dB re 10 cm) should be detected under the same conditions, the maximum detection distance would be approximately 5 m (Fig. 3). With higher frequencies or at less favorable atmospheric conditions, these distances can be even shorter, while if the sonar system’s dynamic range was wider, the range could be considerably extended.

Detection ranges can also be easily estimated using a free webcalculator (Stilz, 2012), which is a computer implementation of the method developed in this paper. Arbitrary parameters of the target GGA, of the bat echolocation system, and of environmental conditions can be specified as defined in this paper, or CGA-parameter-combinations of examined targets can be chosen.

A comparison of three European bats species with different SLs and signal frequencies reveals that the different

signal parameters result in rather big differences in detection distances. For this comparison we use *Nyctalus lasiopterus*, a typical open space forager with a low signal frequency of 18 kHz and a high SL around 111 dB, and *Pipistrellus kuhli*, a bat which forages in open and in edge space and emits signals with a medium SL around 106 dB and a medium frequency of 39 kHz, and *Pipistrellus pygmaeus* which forages closer to edges and emits signals with a low SL around 101 dB and a high frequency around 55 kHz. We used our data to determine the maximal detection distance for a large, medium, and small sized insect with TS of –40, –50, and –65 dB (Houston et al., 2004; Holderied and von Helversen, 2003). We also determined the maximal detection distances for different backgrounds: Mirror, forest, tree, water, and meadow. To demonstrate the effect of SL we determined in each species not only the maximal detection distances for its own DR but also for the DRs of the other species (Table III). The data demonstrate that the acoustic world of bats shrinks strongly with increasing signal frequency, decreasing SL, and with TS in small targets such as prey insects. For instance, the maximal detection distance for a forest edge is at 47.7 m in *Nyctalus lasiopterus* and only at 9.3 m in *Pipistrellus pygmaeus*. Even if we assume that PM would operate with the same dynamic range as NL, the maximum detection distance would only be slightly higher at 11.6 m. A NL foraging for large insects has a maximal range of 9.3 m whereas PM reaches only 1.7 m when foraging for small insects. The strong effect of frequency combined with SL reduction, high humidity, and high temperature gets even more evident when we compare the maximum detection distances of European bats with those of neotropical phyllostomatid bats. If we assume for the phyllostomatid bats a reasonable SL of 80 dB (Brinklov et al., 2009), a DT of 20 dB, a humidity of 100%, a temperature of 28 °C, and frequencies around 80 and 100 kHz we find that the echolocation ranges are again distinctly shorter than in the European bats. For example, the detection ranges for a forest edge are reduced to 3.2 m at 80 kHz and 2.4 m at 100 kHz (Table III).

TABLE III. Estimated target detection ranges [m] based on GGA functions. f = frequency [kHz], DR = dynamic range [dB], F = forest, T = tree, W = water surface, M = meadow. Bold rows: *Nyctalus lasiopterus*, *Pipistrellus kuhli*, *Pipistrellus pygmaeus* (20 °C and 60% humidity) and two phyllostomid bats (28 °C and 100% humidity).

f	DR	Point reflector		Mirror	F	T	W	M	
	TS/ C_1	–40.0	–50.0	–65.0	–6.0	–33.0	–25.0	–4.4	–20.1
	C_2	–40.0	–40.0	–40.0	–20.0	–12.3	–20.5	–17.9	–14.6
18	91	11.3	7.5	3.7	62.7	47.7	41.8	68.6	57.7
18	86	9.2	6.0	2.9	57.3	42.2	36.9	63.1	52.1
18	81	7.5	4.7	2.2	52.0	36.7	32.1	57.6	46.7
39	91	6.8	5.0	2.9	22.6	16.7	16.1	24.1	20.2
39	86	5.9	4.2	2.3	20.9	15.0	14.5	22.4	18.5
39	81	5.0	3.5	1.8	19.2	13.3	12.9	20.7	16.8
55	91	5.5	4.1	2.5	15.8	11.6	11.5	16.8	14.0
55	86	4.8	3.5	2.1	14.7	10.5	10.4	15.6	12.9
55	81	4.1	3.0	1.7	13.6	9.3	9.3	14.5	11.7
80	60	1.6	1.1	0.6	6.0	3.2	3.6	6.4	4.7
100	60	1.4	1.0	0.5	4.5	2.4	2.8	4.7	3.5

V. CONCLUSIONS

The examined backgrounds differed mainly in the vertical offset of their GGA-function, which accounts for the part of energy reflected back by the target and had a range of -33.3 dB to -4.4 dB at 1 m. The slope of the function for the different targets was much more confined to a range of -12.3 to -20.5 dB per tenfold increase in distance. According to this, the reflection properties of the different ensounded targets are more characterized by the energy lost or reflected in the surface than by further energy spreading in the distances recorded.

Atmospheric attenuation is increasing at a constant rate per meter, while geometric attenuation is increasing logarithmically over distance. Thus, the increase of geometric attenuation becomes very low at high distances and eventually atmospheric attenuation will overtake geometric attenuation (Fig. 1). While the geometric attenuation of the echoes for a specific target between 2 and 20 m target distance is changing by only approximately 20 dB, atmospheric attenuation for the full sound traveling distance of 40 m may vary for different call frequencies and atmospheric conditions from approximately 5 dB to more than 200 dB (Fig. 2). Thus, atmospheric attenuation, determined by the combination of call frequency and atmospheric conditions, is dominantly limiting the distance over which audible echoes can be reflected by extended targets to an echolocating bat.

Frequency is the bat's most dominant parameter for the reduction of detection distance. In general, low signal frequency indicates long range and high frequency short range echolocation. Additionally, low frequency bats often forage in open space and have higher SLs which also increases the detection ranges, whereas high frequency bats operate closer to vegetation and have lower SLs which reduces the detection distances. Bats with very high frequencies and very low SLs often live in the tropics where humidity and temperature are very high. These are additional effects which decrease the detection ranges.

ACKNOWLEDGMENTS

We would like to thank the mechanic workshop and the electronic workshop at the University of Tübingen. The project was funded by the Deutsche Forschungsgemeinschaft (SFB 550 and Schn 138/27-1).

Aldridge, H. D. J. N., and Rautenbach, I. L. (1987). "Morphology, echolocation and resource partitioning in insectivorous bats," *J. Anim. Ecol.* **56**, 763–778.

Ayrapetyants, E. S., and Konstantinov, A. I. (1974). *Echolocation in Nature* (Nauka, Leningrad) (in Russian). English transl.: Joint Publications Research Service, Arlington, Virginia, No. 63328, pp. 210–222.

Brinklov, S., Kalko, E. K. V., and Surlykke, A. (2009). "Intense echolocation calls from two 'whispering' bats, *Artibeus jamaicensis* and *Macrophyllum macrophyllum* (Phyllostomidae)," *J. Exp. Biol.* **212**, 11–20.

Denzinger, A., and Schnitzler, H.-U. (2004). "Perceptual tasks in echolocating bats," in *Dynamic Perception—Workshop of the GI Section 'Computer Vision'*, edited by U. J. Ilg, H. H. Bülthoff, and H. A. Mallot (Akademische Verlagsgesellschaft, Berlin), pp. 22–28.

Fenton, M. B., Audet, D., Obrist, M. K., and Rydell, J. (1995). "Signal strength, timing and self-deafening: The evolution of echolocation in bats," *Paleobiology* **21**, 229–242.

Griffin, D. R. (1958). *Listening in the Dark* (Yale University Press, New Haven), 413 pp.

Griffin, D. R. (1971). "The importance of atmospheric attenuation for the echolocation of bats," *Anim. Behav.* **19**, 55–61.

Griffin, D. R., and Buchler, E. R. (1978). "Echolocation of extended surfaces," in *Animal Migration, Navigation and Homing*, edited by K. Schmidt-Koenig and W. T. Keeton (Springer Verlag, Berlin), pp. 201–208.

Griffin, D. R., Webster, F. A., and Michael, C. R. (1960). "The echolocation of flying insects by bats," *Anim. Behav.* **8**, 141–154.

Hartley, D. J. (1989). "The effect of atmospheric sound absorption on signal bandwidth and energy and some consequences for bat echolocation," *J. Acoust. Soc. Am.* **85**, 1338–1347.

Holderied, M. W., Jones, G., and von Helversen, O. (2006). "Flight and echolocation behaviour of whiskered bats commuting along a hedgerow: Range-dependent sonar signal design, Doppler tolerance and evidence for 'acoustic focusing,'" *J. Exp. Biol.* **209**(10), 1816–1826.

Holderied, M. W., and von Helversen, O. (2003). "Echolocation range and wingbeat period match in aerial-hawking bats," *Proc. R. Soc. London, Ser. B* **270**, 2293–2299.

Houston, R. D., Boonman, A. M., and Jones, G. (2004). "Do echolocation signal parameters restrict bats' choice of prey?," in *In Echolocation in Bats and Dolphins*, edited by J. A. Thomas, C. F. Moss, and M. Vater (The University of Chicago Press, Chicago), pp. 339–345.

International Organization for Standardization. (1993). *ISO 9613-1:1993, Acoustics—Attenuation of sound during propagation outdoors—Part 1: Calculation of the Absorption of Sound by the Atmosphere* (American National Standard Institute, New York), pp. 1–30.

Jung, K., Kalko, E. K. V., and von Helversen, O. (2007). "Echolocation calls in Central American emballonurid bats: Signal design and call frequency alternation," *J. Zool.* **272**, 125–137.

Kick, S. A. (1982). "Target detection by the echolocating bat, *Eptesicus fuscus*," *J. Comp. Physiol.* **145**, 431–435.

Kinsler, L. E., and Frey, A. R. (1962). *Fundamentals of Acoustics*, 2nd ed. (John Wiley & Sons, New York), 524 pp.

Lawrence, B. D., and Simmons, J. A. (1982). "Measurements of atmospheric attenuation at ultrasonic frequencies and the significance for echolocation by bats," *J. Acoust. Soc. Am.* **71**, 585–590.

Mohl, B. (1988). "Target detection by echolocating bats," in *Animal Sonar*, edited by P. E. Nachtigall and P. W. B. Moore (Plenum Press, New York), pp. 435–450.

Moss, C. F., and Schnitzler, H.-U. (1995). "Behavioral studies of auditory information processing" in *Hearing by Bats*, edited by A. N. Popper and R. R. Fay (Springer Verlag, New York), pp. 87–145.

Morse, P. M., and Ingard, K. U. (1986). *Theoretical Acoustics* (Princeton University Press, Princeton, NJ), 927 pp.

Neuweiler, G. (1990). "Auditory adaptations for prey capture in echolocating bats," *Physiol. Reviews* **70**, 615–641.

Petrites, A. E., Eng, O. S., Mowlds, D. S., Simmons, J. A., and DeLong, C. M. (2009). "Interpulse interval modulation by echolocating big brown bats (*Eptesicus fuscus*) in different densities of obstacle clutter," *J. Comp. Physiol.* **195**, 603–617.

Ratcliffe, J. M., Jakobsen, L., Kalko, E. K. V., and Surlykke, A. (2011). "Frequency alternation and an offbeat rhythm indicate foraging behavior in the echolocating bat, *Saccopteryx bilineata*," *J. Comp. Physiol. A* **197**(5), 413–423.

Rayleigh, J. W. S. (1896). *The Theory of Sound*, 2nd ed. (MacMillan and Co., Ltd., London), Vol. II, 504 pp.

Schnitzler, H.-U., and Henson, O. W. (1980). "Performance of airborne sonar systems," in *Animal Sonar Systems*, edited by R.-G. Busnel and J. F. Fish (Plenum Press, New York), pp. 109–181.

Schnitzler, H.-U., and Kalko, E. K. V. (2001). "Echolocation by insect-eating bats," *BioScience* **51**, 557–569.

Schnitzler, H.-U., Moss, C. F., and Denzinger, A. (2003). "From spatial orientation to food acquisition in echolocating bats," *Trends Ecol. Evol.* **18**, 386–394.

Skolnik, M. I. (2001). *Introduction to Radar Systems*, 3rd ed. (McGraw-Hill, New York), 772 pp.

Sokolov, B. V. (1972). "Interaction of auditory perception and echolocation in bats Rhinolophidae during insect catching," *Vestn. Leningr. Univ. Ser. Biol.* **27**, 96–104 (in Russian).

Stilz, W.-P. (2012). "Echolocation range calculator," <http://www.biosonarlab.uni-tuebingen.de/rangecalculator/index.html> (Last viewed July 26, 2012).

Surlykke, A., and Kalko, E. K. V. (2008). "Echolocating bats cry out loud to detect their prey," *PLoS One*, **3**(4), e2036.

Urlick, R. J. (1983). *Principles of Underwater Sound*, 3rd ed. (McGraw-Hill Co., New York), 423 pp.